

# Supporting Information for “On the origin of seismic anisotropy in the shallow crust of the Northern Volcanic Zone, Iceland”

C. A. Bacon<sup>1</sup>, J. Johnson<sup>2</sup>, R. S. White<sup>1</sup>, N. Rawlinson<sup>1</sup>

<sup>1</sup>Department of Earth Sciences, University of Cambridge, UK

<sup>2</sup>School of Environmental Sciences, University of East Anglia, UK

## Contents of this file

1. Captions for Datasets S1 to S2
2. Table S1
3. Figures S1 to S3

## Introduction

This supporting document contains some additional examples of shear-wave splitting measurements and the results of the parameter trials used for the regridding of shear-wave splitting results as outlined in Sections 3.2.1 and 3.2.2. In addition, there is a table that provides the parameters used by MFAST and the captions for datasets S1 and S2, which can be downloaded separately.

**Data Set S1.** The input file used for the Coulomb stress modeling outlined in Section 4.2.

---

X - 2

:

**Data Set S2.** The result file containing all of the splitting measurements used in this study.

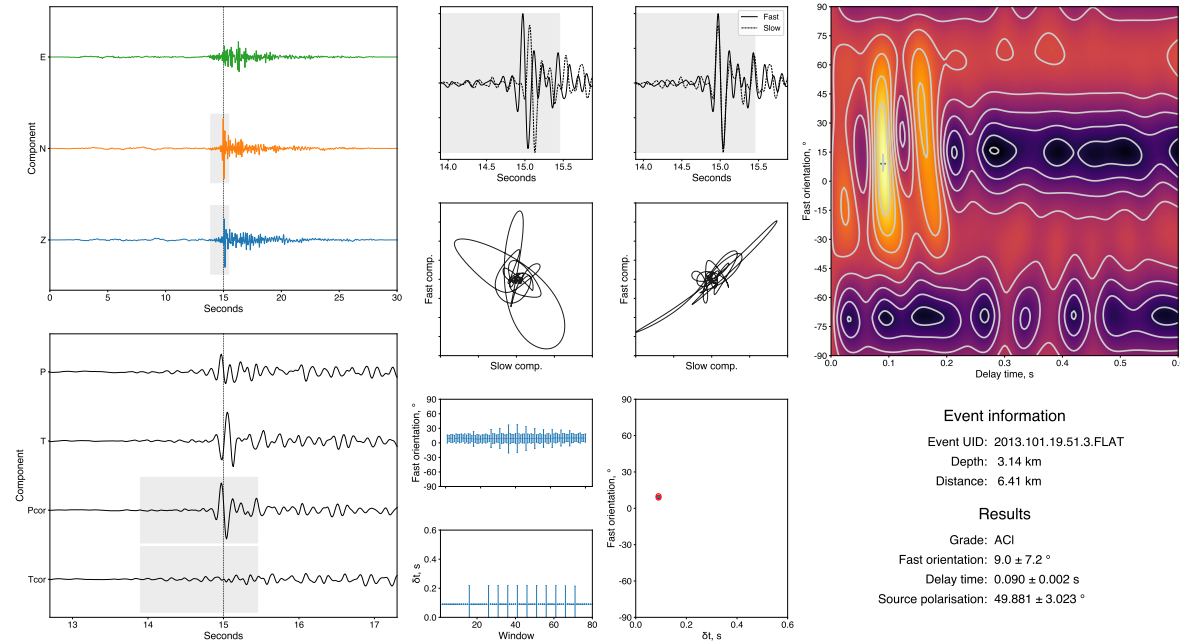


**Figure S1.** Example of a good splitting measurement at FLAT for a repeating earthquake (multiplet)—see Figure S2. (a) shows the raw data for the East (green), North (orange), and Vertical (blue) components. (b) shows a zoom in around the S phase arrival rotated onto the nominal ‘radial’ (P) and ‘transverse’ (T) axes before and after correction for splitting. Panels (c) and (d) show the phase arrivals rotated onto the ‘fast’ and ‘slow’ axes before and after correction, with (e) and (f) showing the corresponding particle motion. There is a clear linearisation of the particle motion of the horizontal components and removal of energy from the transverse component. Panels (g) - (i) show the results of the multiple window trials and the cluster analysis. Finally, (j) shows the resultant grid of the minimised eigenvalue. The blue cross denotes the optimal  $(\delta t, \phi)$  pair.



June 28, 2021, 12:23pm

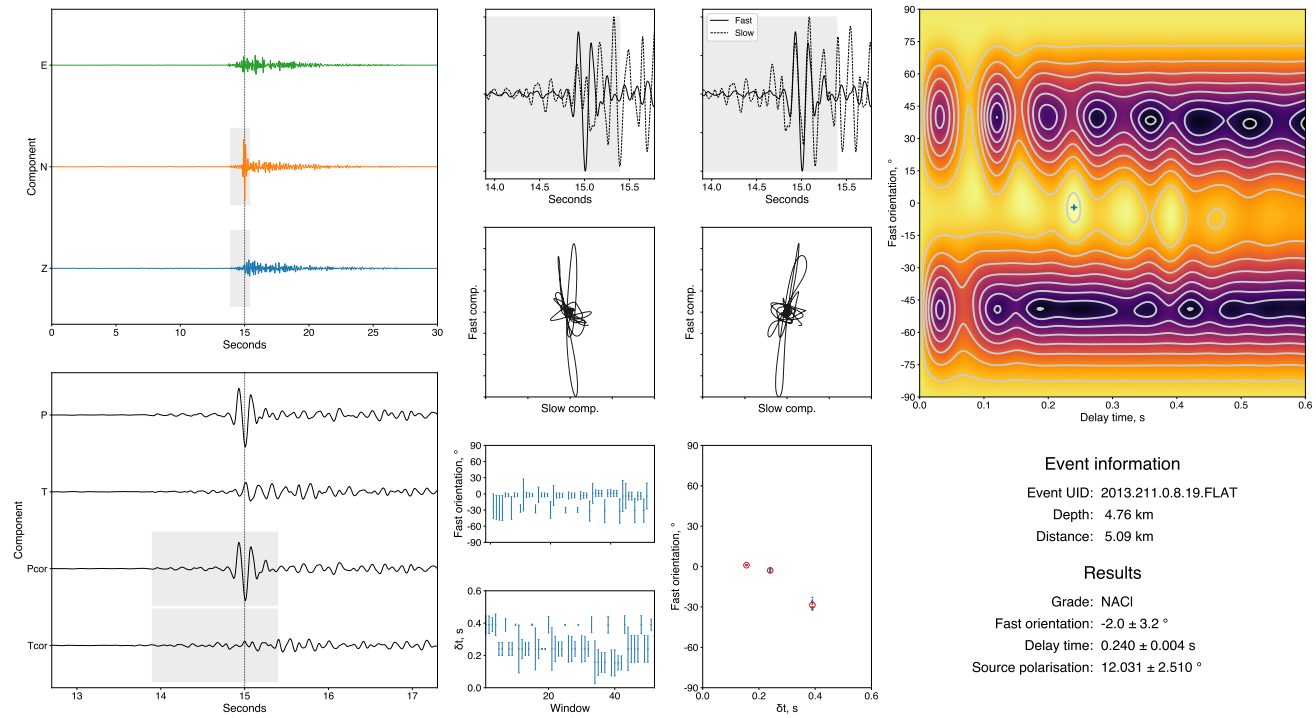


Figure S3. Example of a null splitting measurement at FLAT. Panels the same as Figure S1.

June 28, 2021, 12:23pm

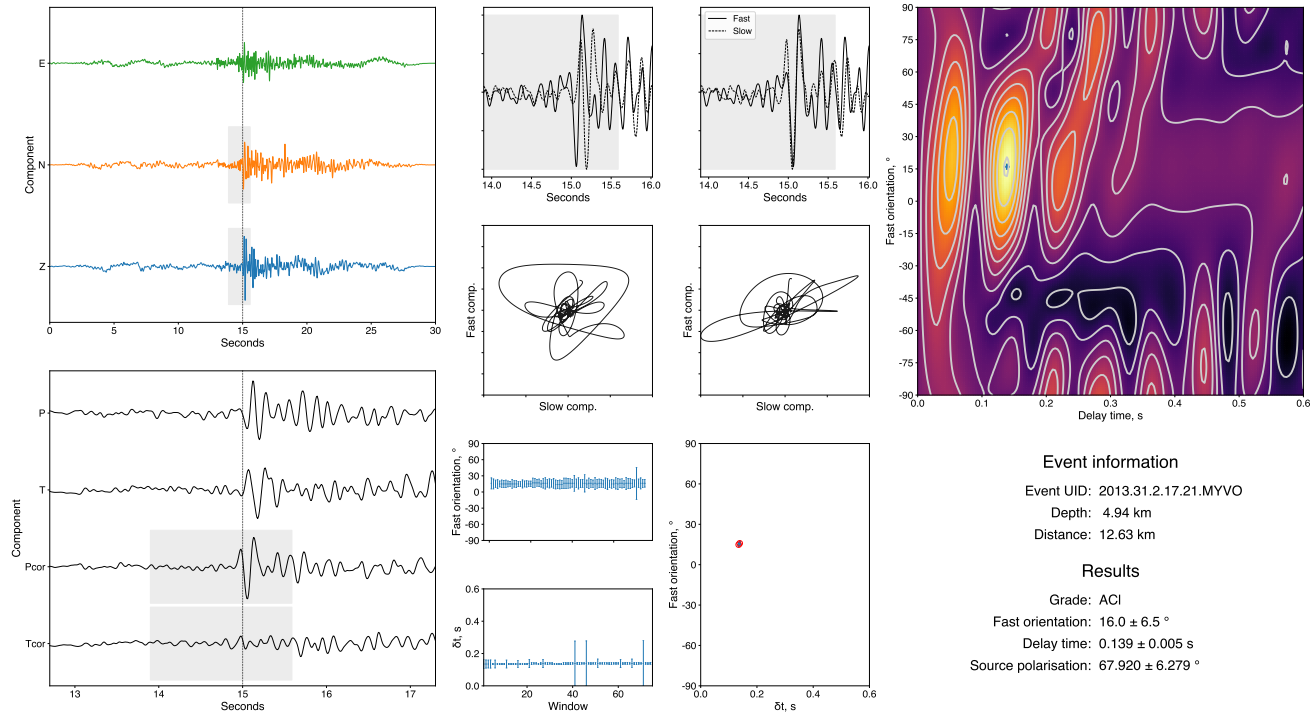
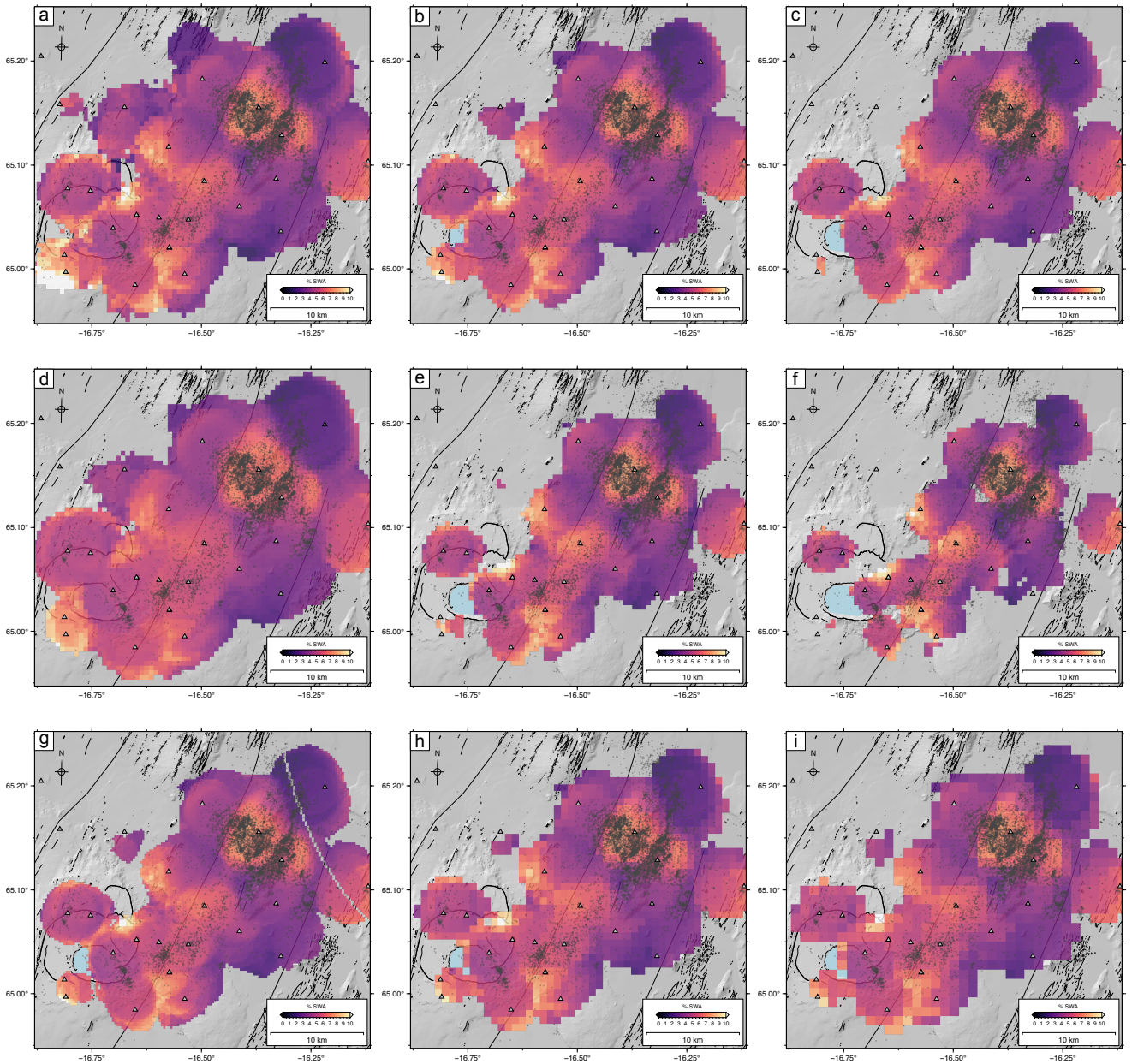


Figure S4. Example of a good splitting measurement at MYVO. Panels the same as Figure S1.

<b>Parameter name</b>	<b>Description</b>	<b>Value</b>
<i>nwbeg</i>	Number of measurement window start times tested	5
<i>nwend</i>	Number of measurement window end times tested	16
<i>dt_beg</i>	Time step size between window start times	0.2
<i>dt_end</i>	Time step size between window end times	0.0158276
<i>dtlag_max</i>	Maximum allowable error in tlag for inclusion in clustering	0.144823
<i>dfast_max</i>	Maximum allowable error in fast for inclusion in clustering	40
<i>t_off_beg</i>	First time of start window	0.3
<i>t_off_end</i>	First time of end window	0.279293
<i>tlag_scale</i>	Maximum time lag	0.579293
<i>fast_scale</i>	Maximum fast direction	180
<i>max_no_clusters</i>	Maximum number of clusters to test during cluster analysis	15
<i>nmin</i>	Minimum number of points in an acceptable cluster	5

**Table S1.** Table giving the MFAST parameter values used for this study.



**Figure S5.** Shear wave anisotropy (SWA) re-gridding parameter trials. Each row shows a different parameter variation: a–c show variations in the minimum number of observations required per cell, with values of 3, 8, and 15 from left to right; d–f show variations in the width of the Gaussian kernel used for smoothing the data, with values of 1500, 2000, and 3500 from left to right; g–i show variations in the grid cell size with values of  $0.25 \times 0.25 \text{ km}^2$ ,  $0.75 \times 0.75 \text{ km}^2$ , and  $1 \times 1 \text{ km}^2$  from left to right. There are no notable differences between the trials, suggesting that the features observed are robust.

June 28, 2021, 12:23pm

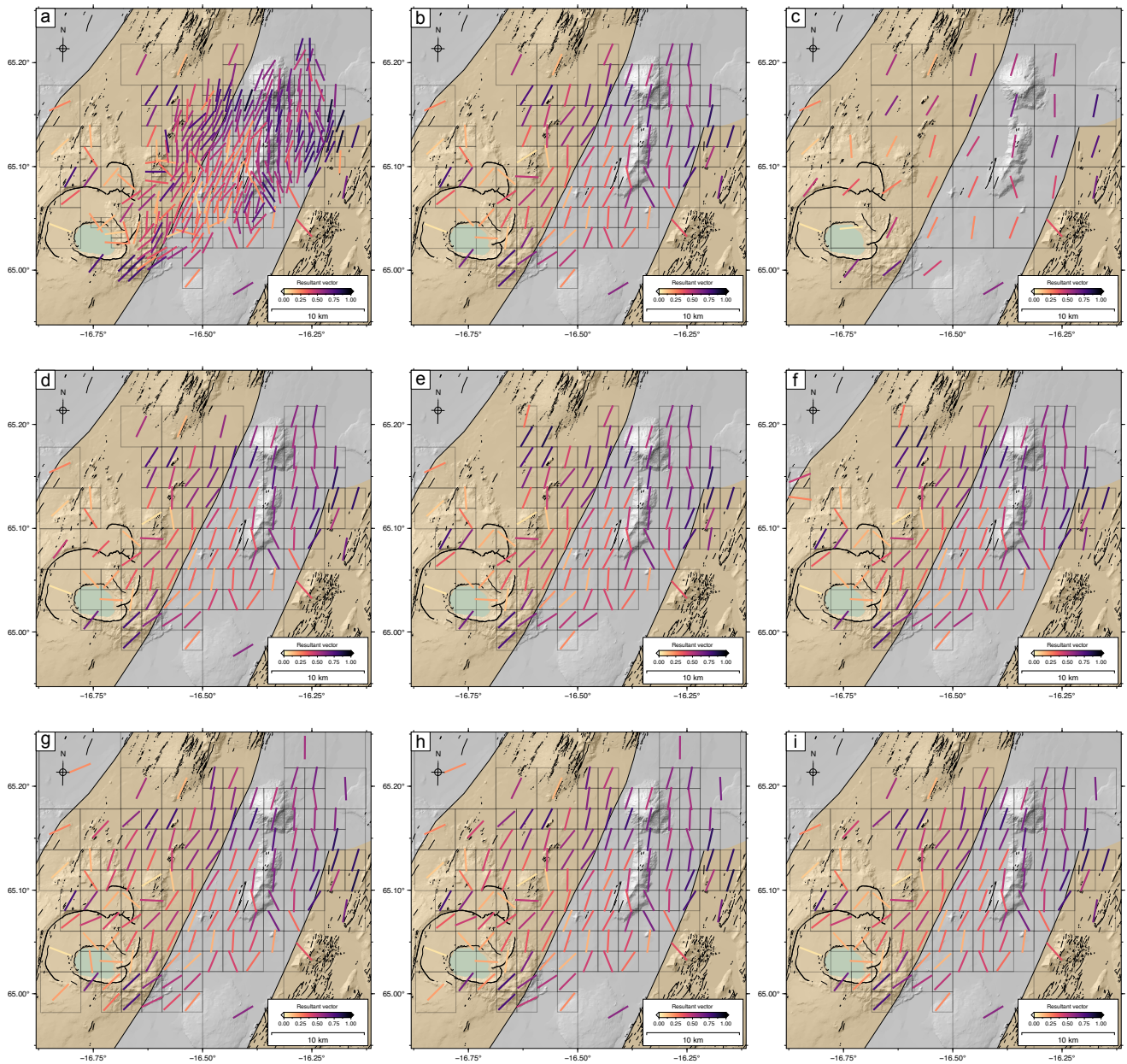


**Figure S6.** Fast polarization ( $\phi$ ) re-gridding parameter trials. Each row shows a different parameter variation: a–c show variations in the minimum cell size, with values of  $1 \times 1 \text{ km}^2$ ,  $1.5 \times 1.5 \text{ km}^2$ , and  $3 \times 3 \text{ km}^2$  from left to right; d–f show variations in the maximum number of observations before a cell is subdivided,  $n_{max}$ , with values of 100, 150, and 250 from left to right; g–i show variations in the minimum number of observations required for a cell to be retained,  $n_{min}$ , with values of 20, 30, and 50 from left to right. There are no notable differences between the trials, suggesting that the features observed are robust.

June 28, 2021, 12:23pm

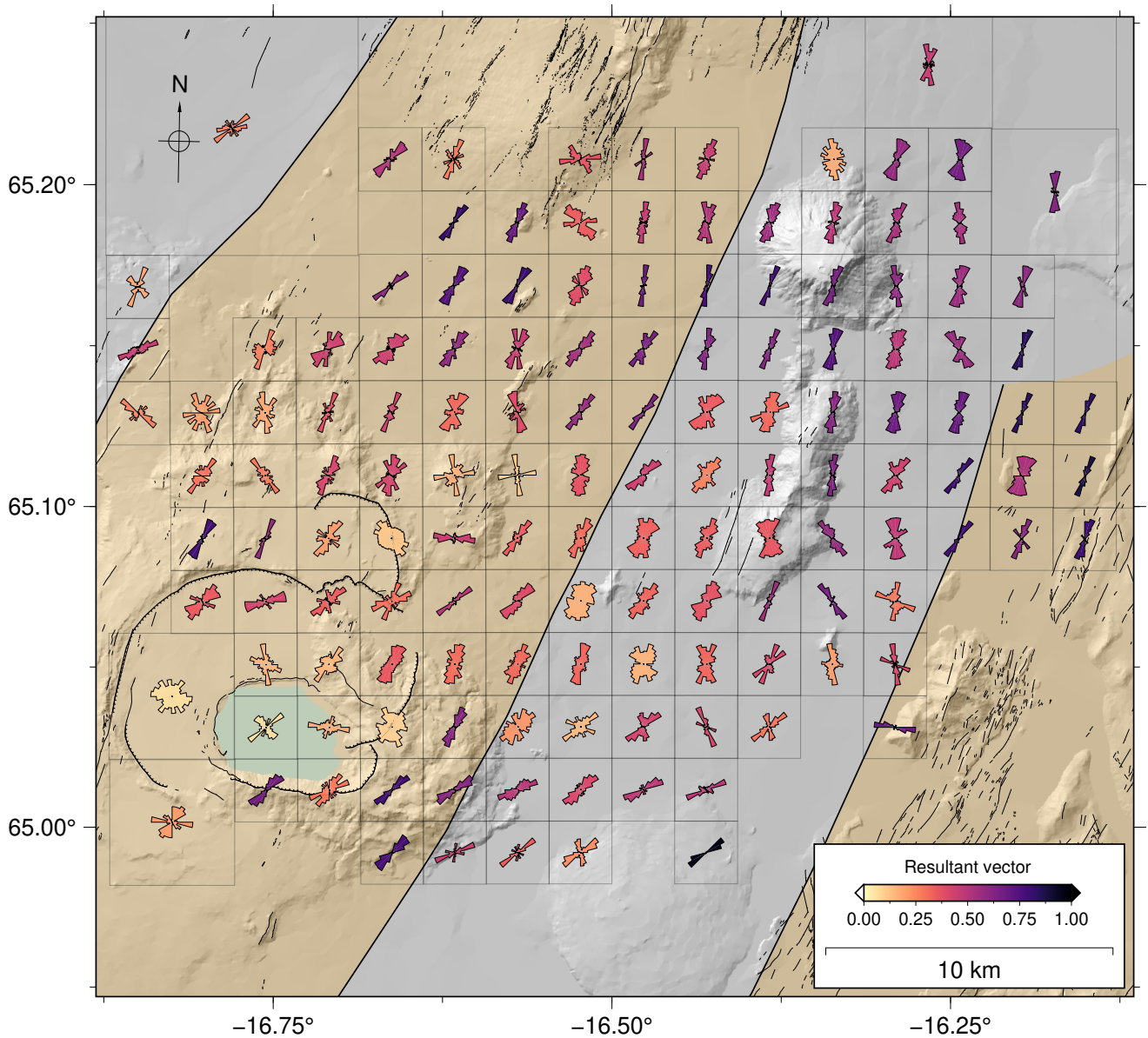


**Figure S7.** Lateral variations in observed fast axis orientations,  $\phi$ . The observations have been assigned to the midpoint between source and receiver, then re-gridded using a quadtree method. The resultant grid is plotted using faint black lines. Within each cell, the rose diagram shows the distribution of fast axis orientation measurements, colored by the ‘resultant vector’ which is a measure of dispersion/coherence of the orientation data. Darker colors indicate stronger coherence.